

Efficient Removal of Diclofenac from Pharmaceutical Wastewater Using Impregnated Zeolite Catalyst in Heterogeneous Fenton Process

M. Rostamizadeh^{a,b,*}, H. Jalali^{a,b}, F. Naeimzadeh^c and S. Gharibian^{a,b}

^aDepartment of Chemical Engineering, Sahand University of Technology, Sahand New Town, East Azerbaijan, Iran

^bEnvironmental Engineering Research Center, Department of Chemical Engineering, Sahand University of Technology, Sahand New Town, Iran

^cFaculty of Pharmacy, Tabriz University of Medical Sciences, Tabriz, East Azerbaijan, Iran

(Received 18 August 2018, Accepted 17 November 2018)

In this study, we report removal of Diclofenac (DCF) through heterogeneous Fenton process using Fe-ZSM-5 catalyst. The parent catalyst was prepared by hydrothermal technique. Fe species were introduced by wet impregnation. Characterization of the catalysts was carried out using XRD, FT-IR, FE-SEM, N₂ adsorption-desorption, NH₃-TPD, and acidimetric-alkalimetric titration. The bimetallic catalyst had the high crystallinity (81.2%), specific surface area (291.8 m² g⁻¹) and uniform spherical morphology. Effect of pH, temperature, catalyst concentration, and H₂O₂ concentration on DCF removal efficiency was investigated. The results showed that the optimum conditions were reaction temperature of 25 °C, H₂O₂ concentration of 10 mM, pH level of 3, and catalyst concentration of 2 g l⁻¹ which resulted in the highest DCF removal (97%). No significant change was observed in the catalytic performance when it was applied in the sequence cycles at the optimum reaction conditions. The prepared catalyst showed the high potential for the treatment of the pharmaceutical wastewater due to the high efficiency and stability.

Keywords: Advanced oxidation process, Heterogeneous Fenton, Diclofenac, Catalyst, Zeolite

INTRODUCTION

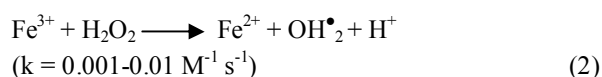
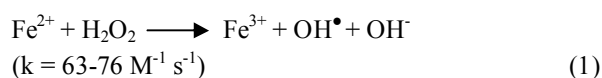
Complicated and non-biodegradable compounds available in municipal and industrial wastewaters have turned them very critical environmental issues. Pharmaceutical industry is one of the main sources of the environment pollution owing to the expired drugs as well as drug discharge from factory [1]. Pharmaceuticals are consumed by humans and animals which are usually metabolic resistance and part of them are excreted through urine. Among the different pharmaceuticals, non-steroidal anti-inflammatory drugs (NSAIDs) are critically environmental issues owing to their extensive availability. Diclofenac (2-(2,6-dichlorophenylamino) phenyl acetic

acid, DCF) is a common NSAID with annual sale of more than 100 tons [2]. DCF is consumed as analgesic, antiarthritic and antirheumatic agent. DCF is relatively stable and resists to biodegradation so ubiquitously exists in the environment. Very low concentration of DCF in the range of μg l⁻¹ causes serious adverse effects on the aquatic living life and human life [3-5]. Although, large quantities of DCF are degraded through solar radiation at surface water or through unit operations in wastewater treatment plants, the remaining quantities are considerable.

The current wastewater treatments include membrane separation [6,7], evaporation [8] and precipitation [9] which cannot remove total amount of resistive pollutions [10]. Therefore, efforts on the field of water purification focus on conventional and advanced oxidation processes (AOPs). AOPs include Fenton [11,12], Fenton like reactions [13], Electro-Fenton [14-16], degradation by O₃ [17], O₃/H₂O₂

*Corresponding authors. E-mail: Rostamizadeh.m@gmail.com

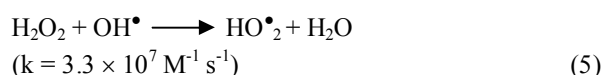
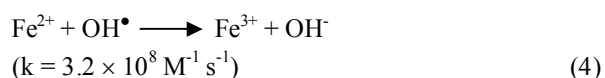
[18], UV irradiation [19], sonolysis [20] and hybrid systems [21]. AOPs are continuous production of reactive hydroxyl oxidant (hydroxyl radical OH^\bullet ; $E_0: 2.76\text{V}$). In classical Fenton reaction, hydroxyl generation is carried out through activation of H_2O_2 by ferrous (Fe^{2+}) ions (*i.e.* Eqs. (1)-(2)) [22].



Hydroxyl radicals then react with organic substrate and oxidize it (*i.e.* Eq. (3)) [23].



Side reactions can be enhanced by inappropriate operational conditions including neutral pH level or excess concentration of homogenous ferrous ion (*i.e.* Eqs. (4)-(6)) resulting in lower oxidizing power or production of ferric hydroxide [24,25].



Thus, the control of the reaction conditions has a significant impact on the oxidation efficiency. Fe^{2+} ion is catalyst of Fenton reaction which is either homogenous (*i.e.* dissolution of iron salts like FeSO_4 in aqueous solution resulting aqueous Fe^{2+}) [26,27] or heterogeneous (through immobilizing Fe into porous support materials) [14]. Pillared clays, zeolites, silica, iron oxide, and natural iron minerals have been investigated in the heterogeneous Fenton reaction [28]. The structural matrix of the supported catalysts provides several advantages such as high specific surface area [29], effective controlling of iron leaching, less

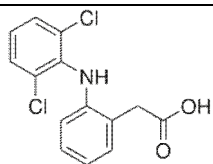
generation of iron sludge, low catalyst cost, and high stability of catalyst [28,30]. Bae *et al.* [3] investigated oxidation of DCF using pyrite as catalyst. They reported that continuous dissolution of aqueous Fe^{2+} from pyrite catalyst led to the complete degradation of DCF in the appropriate range of pH level (3-4). Epold *et al.* [31] investigated heterogeneous and homogenous degradation of DCF by photolysis. Heterogeneous reaction was catalyzed using goethite, and homogenous reaction was catalyzed by Fe^{2+} ions. The results showed that nearly complete degradation efficiency was obtained by heterogeneous Photo-Fenton reaction (3.8 mM H_2O_2 , pH = 7) after 120 min, while, at the same reaction conditions, homogenous reaction had 95% degradation efficiency. Perisic *et al.* [2] investigated the removal of DCF using UV-A/ $\text{FeZSM5}/\text{H}_2\text{O}_2$ process. Their proposed system resulted in 98% DCF removal after 120 min of photo-Fenton reaction at pH = 4, $[\text{H}_2\text{O}_2] = 50 \text{ mM}$, and $[\text{Fe}]_{\text{Fe-ZSM-5}} = 2 \text{ mM}$. Salaeh *et al.* [32] investigated DCF removal by Photo-Fenton reaction catalyzed by $\text{TiO}_2/\text{Fe-ZSM-5}$. They concluded that DCF degradation pathway included adsorption on heterogeneous catalyst surface and consequent degradation. They reported nearly complete DCF removal in 180 min of reaction at pH = 4 and $[\text{H}_2\text{O}_2] = 3.88 \text{ mM}$. As the best of our knowledge, there is no report on the application of Fe-ZSM-5 catalyst for DCF removal through Fenton reaction. The main objective of this study is to synthesize and characterize the Fe-ZSM-5 catalyst and their application in heterogeneous Fenton reaction for DCF removal. The effects of pH level of wastewater, temperature, catalyst concentration, and H_2O_2 concentration are also studied.

EXPERIMENTAL

Materials

The chemicals utilized in this study are silicic acid ($\text{SiO}_2 \cdot x\text{H}_2\text{O}$, >99 wt.%), sodium aluminate (NaAlO_2 , Al_2O_3 wt.% = 55), iron nitrate ($\text{Fe}(\text{NO}_3)_3 \cdot 9\text{H}_2\text{O}$, 99 wt.%), tetrapropyl ammonium bromide (TPABr, $\text{C}_{12}\text{H}_{28}\text{BrN}$, >99 wt.%), ammonium nitrate (NH_4NO_3 , 99 wt.%), sodium hydroxide (NaOH , 99.6 wt.%), sulfuric acid (H_2SO_4 , 98 wt.%), and hydrogen peroxide (H_2O_2 , 35 wt.%) which were supplied from Merck company (Germany). Diclofenac sodium salt ($\text{C}_{14}\text{H}_{10}\text{Cl}_2\text{NNaO}_2$) was kindly denoted by

Table 1. General Information of DCF

Structure	Formula	Molar mass (g mol ⁻¹)	Maximum absorbance (nm)
	C ₁₄ H ₁₁ Cl ₂ NO ₂	296.148	275

Zahravi pharmaceutical Company (Iran). General information and specifications of DCF are shown in Table 1.

Catalyst Preparation

Parent HZSM-5 catalyst was synthesized using hydrothermal method [33,34]. A solution with molar composition of 20SiO₂:0.05Al₂O₃:3TPABr:1.5Na₂O:200H₂O was stirred mechanically for 3 h. The pH level of solution (10.5) was adjusted by addition of sulfuric acid. Na-ZSM-5 crystals were prepared through crystallization in static stainless-steel Teflon-lined autoclave at 180 °C and autogenous pressure for 48 h. The recovered powder was dried at 105 °C overnight. Then, the powder was calcined in muffle furnace at 530 °C for 12 h with heating rate of 3 °C min^{-surf1}. In order to obtain the H-form of the catalyst, Na-ZSM-5 was ion-exchanged four times using NH₅NO₃ solution (1 M) at 90 °C and continuous agitation for 10 h. The powder was then dried at 105 °C for 12 h followed by calcination at 530 °C for 12 including heating rate of 3 °C min⁻¹. Wet impregnation of parent catalyst resulted in the bimetallic catalyst (Fe1.0-ZSM-5) including iron promoter (1%wt.). The multi-step impregnation was in a rotating evaporator as follow [35]:

(i) 65 °C and 300 mmHg for 60 min, (ii) 70 °C and 250 mmHg for 30 min, (iii) 70 °C and 200 mmHg for 30 min, (iv) 75 °C and 200 mmHg for 30 min, (v) 75 °C and 180 mmHg for 30 min. After impregnation, the catalyst was dried overnight at 105 °C which followed by calcination at 530 °C (3 °C min⁻¹) for 12 h.

Catalyst Characterization

X-ray diffraction (XRD) experiments were carried out with a D8 Advance Bruker AXS X-ray diffractometer with

Ni-filtered Cu K α radiation ($\lambda = 0.15418$ nm). 2 θ variations were recorded in the range of 4-50° at 40 kV. Filed-emission scanning electron microscopy (FESEM) images were taken by A KYKY (Model, EM3200) equipment at a potential difference of 26 kV. Transmission electron microscopy (TEM) was performed on keV80 (Model, EM900) instrument. Acidity of catalysts were measured by temperature programmed desorption of ammonia (NH₃-TPD, micromeritics, USA, equipped with an on-line TCD detector) method. In this method, 53.6 mg of each catalyst sample was pretreated at 550 °C for 4 h. The powders were saturated with NH₃ for 1 h in the micro reactor and helium flow passed over the sample with a heating rate of 10 °C min⁻¹. The range of desorption temperature was 100-700 °C.

The textural properties were measured using the N₂ adsorption-desorption technique at -196.2 °C (Quantachrome, USA). Prior to Brunauer-Emmet-Teller (BET) specific surface area measurements, the powders were degassed at 300 °C for 3 h. The total specific surface area (SBET) and total volume (V_{total}) were calculated according to the BET isothermal equation and the nitrogen adsorbed volume at P/P₀ = 0.99, respectively. The t-plot method calculates the micropore volume (V_{micro}). The mesopore volume (V_{meso}) is the difference between the calculated total data and the corresponding micropore data. Fourier transform infra-red (FT-IR) analysis was conducted using a Nexus Model Infrared Spectrophotometer (Nicolet Co, USA) at the resolution of 4 cm⁻¹. We prepared self-supported wafer containing 1 wt.% of the powder in KBr. Acidimetric-alkalimetric titration method was used to determine the point of zero charge (pHpzc) for the catalyst. HCl, NaOH and NaCl were used as acid, base, and electrolyte, respectively [36]. Different vials were filled

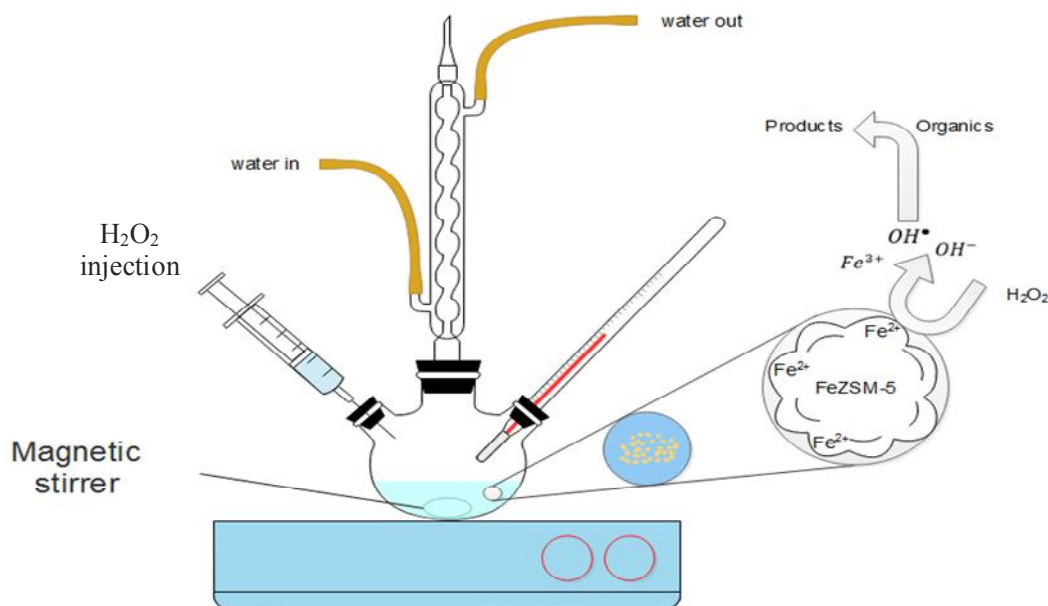


Fig. 1. Schematic of the heterogeneous Fenton process.

with 50 ml of 0.01 M NaCl aqueous solution and pH was adjusted separately using either with 0.01 M HCl or 0.01 M NaOH aqueous solutions. Afterwards, 100 mg of the catalyst was added to each vial and after 24 h of shaking, final pH value was measured [37]. Spectrophotometric measurements of DCF concentration were determined using a UNICO model UV-2100 spectrophotometer (USA).

Fenton Process

Figure 1 represents schematic of the heterogeneous Fenton process. Reaction medium was 50 ml of the synthetic wastewater (30 ppm of DCF in deionized water) and pH level of the solution was adjusted to 3, 5 and 7 by 0.1 M H₂SO₄ and 0.01 M NaOH solution for investigating the effect of operational solution pH. Fe1.0-ZSM-5 catalyst was added to the solution without any stirring and H₂O₂ was injected just after addition of catalyst to prevent any error due to adsorption of DCF on Fe1.0-ZSM-5 particles. Different concentrations of Fe1.0-ZSM-5 catalyst (0, 2, 4, and 6 g l⁻¹) and H₂O₂ (10, 50, and 100 mM) was added in order to investigate the effect of operational parameters. Rapidly, after H₂O₂ injection, magnetic stirrer was turned on in order to homogenize the reaction medium. This point was considered as a starting point for the reaction [11,14].

Samples were taken every 15 min and DCF concentration was determined by UV-Vis spectrophotometer at 275 nm. Removal efficiency was calculated using Eq. (7) [14]:

$$\%DCF\ removal = \frac{C_0 + C_t}{C_0} \times 100 \quad (7)$$

where C_0 and C_t are the DCF concentration in initial wastewater and sample, respectively.

RESULTS AND DISCUSSION

Catalyst Characterization

The catalysts include MFI-structure of ZSM-5 in consistent with standard ZSM-5 (JCP:42-23) (Fig. 2) [38]. The relative crystallinity of the catalyst is the ratio of the peak area located at $2\theta = 22.5-24.5^\circ$ compared to the parent catalyst (Fig. 3). The Fe1.0-ZSM-5 catalyst has the low relative crystallinity compared to that in the parent catalyst which is in agreement with an amorphous peak located at $2\theta = 25.5-27^\circ$. This can be explained by slight framework defects owing to dealumination through the impregnation process which supports the shifted peak positions (Fig. 2). Rebrov *et al.* [39] reported that dealumination changed peak

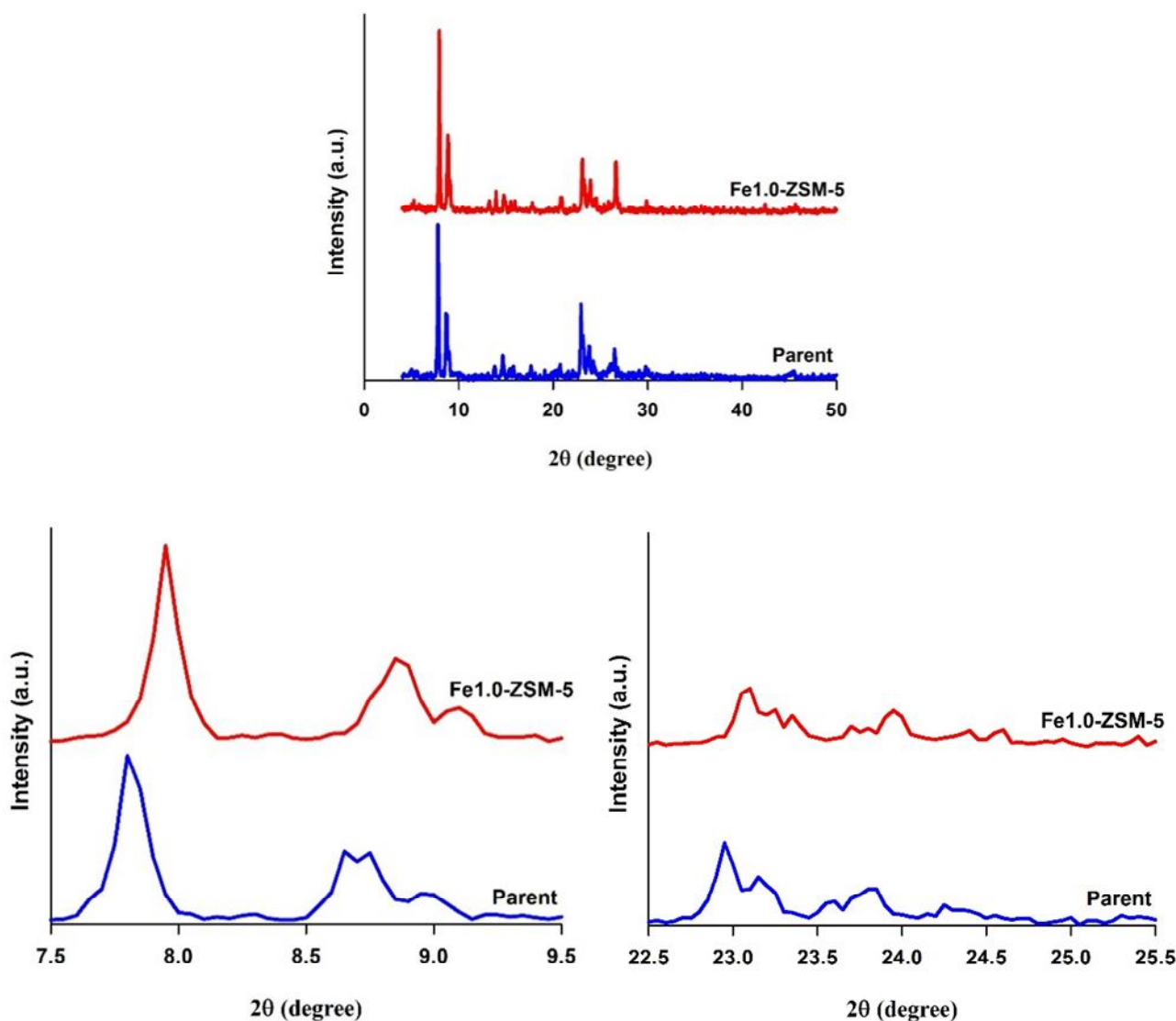


Fig. 2. XRD pattern of the catalysts.

position toward the high 2θ values as the result of slight framework damage. Lack of any peaks related to Fe species indicates the uniform dispersion of the promoter in the catalyst structure. The surface morphology of the catalysts is microspherical aggregation (Fig. 4). It is noticeable that the similar surface morphology and particle size distribution of the bimetallic and parent catalysts show no significant morphology change through the impregnation which agreed with the XRD results. FE-SEM images of the individual microspheres revealed that the microspheres were formed by the aggregation of the nanocrystals (Fig. 4) [35,40].

N_2 adsorption-desorption of the catalysts are a combination of isotherm types I and IV (Fig. 5a). The rectangular type H4 hysteresis loops at the high relative pressure ($P/P_0 = 0.5-0.95$) reveals the mesoporous structure as a result of the capillary condensation [41]. This can be attributed to nitrogen sorption or adsorption by mesoporous structure of interparticle spaces due to the crystalline agglomerates [42]. The high adsorption volume at the very low relative pressure ($P/P_0 = 0.1$) indicates the microporous structures [43]. The pore size distribution of the catalysts shows the formation of the mesoporous structure (Fig. 5b).

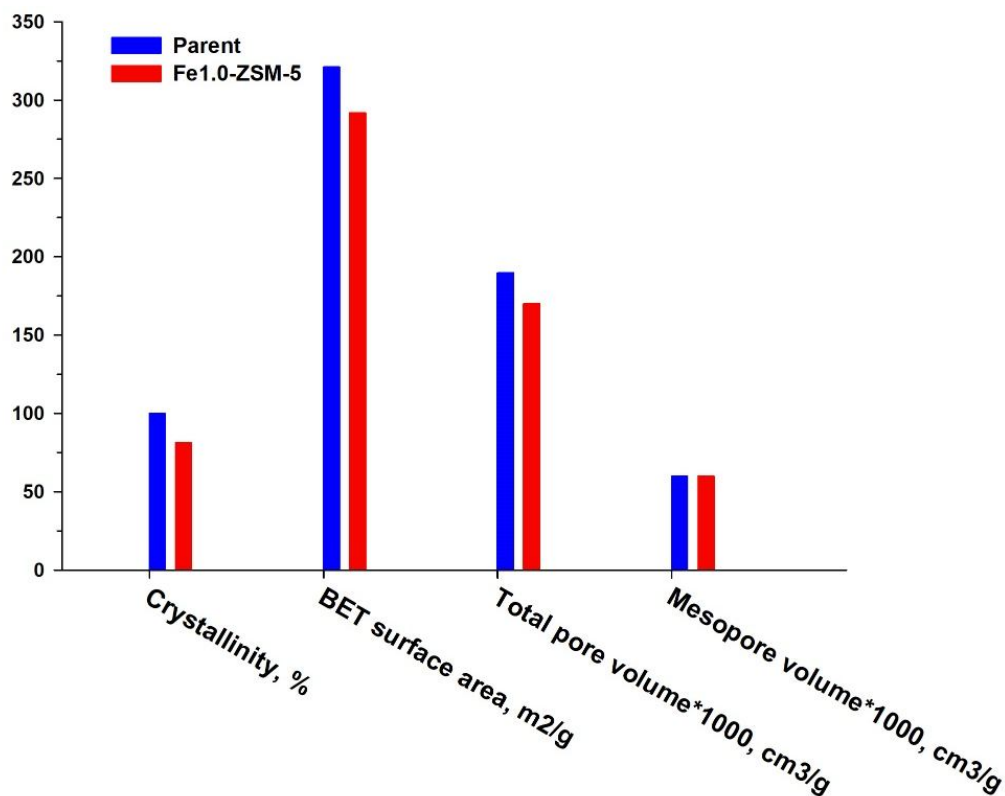


Fig. 3. Textural properties of the catalysts.

The catalysts have the major pore diameter of 1.70 nm. The calculated textural data show the high specific surface area and total pore volume (Fig. 5). The reduction of BET specific surface area and pore volume for the bimetallic catalyst are attributed to the slightly micropore damage or pore blockages. Carbal de Menezes *et al.* [44] reported dealumination and mesopore generation through the impregnation of ZSM-5. The results are in consistent with the XRD results.

Figure 6 shows FT-IR spectra of the catalysts which were recorded in the range of 400-4000 cm^{-1} . The bands near 450 cm^{-1} is assigned to internal SiO_4 and AlO_4 tetrahedral. ZSM-5 zeolite with five membered rings is detected by the band around 550 cm^{-1} . FT-IR spectra in the range of 3500-3800 cm^{-1} represent the surface hydroxyl groups. FT-IR bands at *ca.* 3610 cm^{-1} and 3680 cm^{-1} are attributed to the vibration of bridging Si-OH-Al [45]. Extra-framework aluminum species (Al-OH) in the catalysts lead to the band at 3680 cm^{-1} [46,47].

The NH_3 -TPD measurements result in the similar

patterns for the catalysts including different strength and amount of the acid sites (Fig. 7a). The weak and strong acid sites in the catalysts are characterized by the two desorption peaks at temperature ranges of 130-280 $^{\circ}\text{C}$ and 300-500 $^{\circ}\text{C}$, respectively. The peak area determines the concentration of acid sites (Fig. 7b). The parent catalyst has the equal amount of strong and weak acid sites (0.53 $\text{mmol NH}_3 \text{g}^{-1}$). The impregnation reduces the acidity of the catalysts owing to the interaction of Fe species with zeolite framework. This phenomenon can be explained by the pore blocking and neutralization of the surface acid sites with the promoter [48]. The smaller effective ionic radii of Fe ion (around 0.77 \AA [49]) permits the diffusion of the promoter species inside of ZSM-5 channels (diameter of 5.5 \AA) and interaction with internal acid sites. Acidimetric-alkalimetric titration method for the both parent and bimetallic catalyst determines pH_{pzc} equal to 3.6 and 4, respectively. The pH_{pzc} increase for the Fe1.0-ZSM-5 catalyst is in consistent with the results of NH_3 -TPD which shows the acidity reduction through the impregnation. In fact, Fe promoter through the impregnation

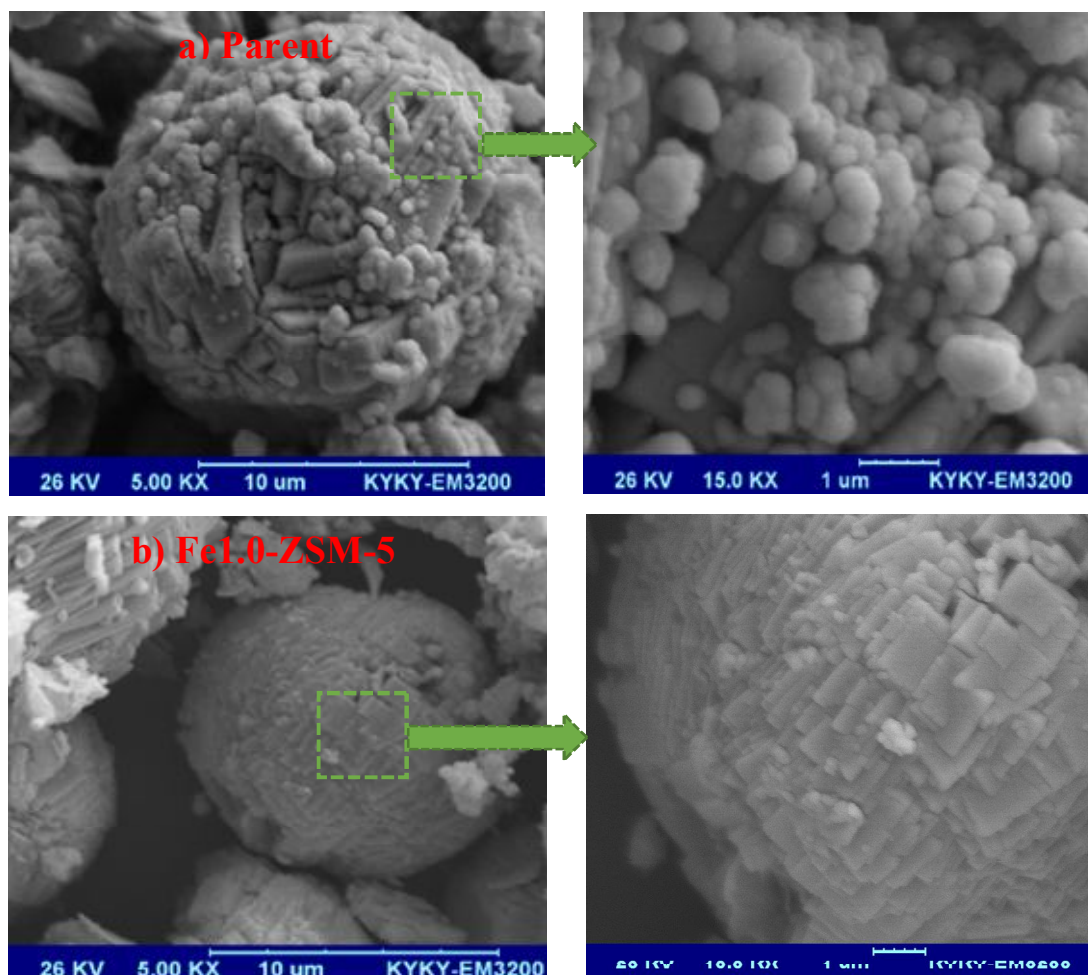


Fig. 4. FE-SEM image of the catalysts a) parent b) Fe1.0-ZSM-5.

hides some Al sites (acid sites) from accessible surface [50]. The surface hydroxyl groups (OH), either as Brønsted acid site or basic site [51], attain positive charge (excess of protons) at $\text{pH} < \text{pH}_{\text{pzc}}$ and negative charge (lack of protons) at $\text{pH} > \text{pH}_{\text{pzc}}$ which influences adsorption capacity of the catalyst at different pH levels.

Catalytic Performance

Effect of pH level. It is well known that the optimum pH level for Fenton and Fenton like processes is in the range of 2-5 [52]. This can be related to the reduced reactivity of H_2O_2 with Fe ion as result of its stabilization through the formation of oxonium ion (H_3O_2^+). The low pH level favors the high DCF removal efficiency (Fig. 8).

The highest efficiency (92%) is obtained at $\text{pH} = 3$. This phenomenon can be explained by the only pK_a value of DCF which is equal to 4.15 [53]. At any pH level above this value, DCF molecules are dissociated into anionic forms in aqueous solutions [54]. However, at $\text{pH} = 3$, DCF molecules have neutral form and the catalyst surface attains a positive charge ($\text{pH} < \text{pH}_{\text{pzc}}$). Therefore, electrostatic interactions do not occur and the removal is mainly occurred by degradation which is predominant over adsorption [55]. This mechanism includes formation of OH^\bullet through Fenton reaction between H_2O_2 and iron ions inside the catalyst structure and diffusion of the formed OH^\bullet into the bulk of the reaction medium where they react with DCF molecules. According to Fig. 8, the DCF removal has decreased from

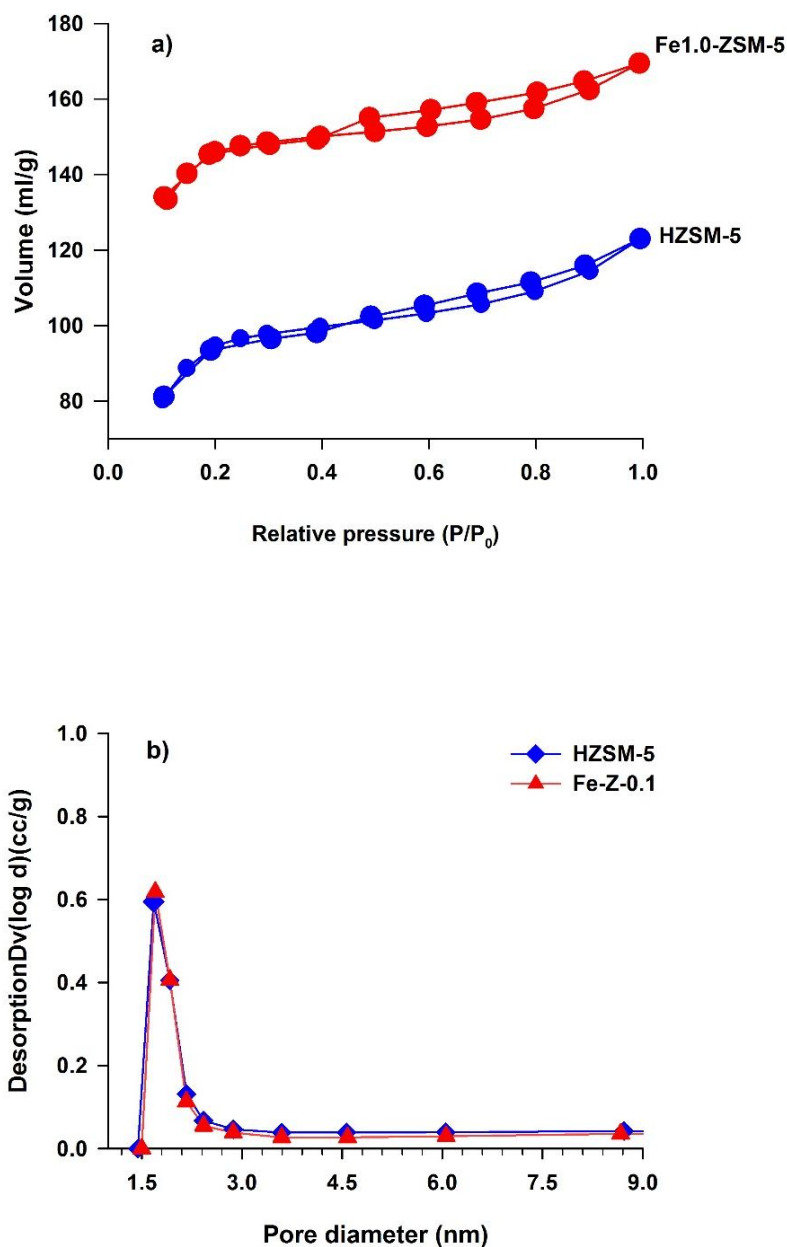


Fig. 5. (a) N₂ adsorption-desorption isotherm and (b) pore size distribution of the catalysts.

92% at pH = 3 to 83% at pH = 5. However, this reduction in DCF removal is more significant at pH = 7. Contrary to the previous case, DCF molecules have anionic form at pH levels above pK_a of DCF. Hence, the negative charged surface of the catalyst (pH > pH_{pzc}) and anionic DCF molecules are subjected to electrostatic repulsion. It is reported that van der Waals and cationic exchange effects

overcome the electrostatic repulsion which lead to adsorption of DCF molecules on the catalyst [36]. These results are in consistent with the results of Perisic *et al.* [2] who reported the negligible adsorption of DCF on Fe-ZSM-5 zeolite at pH level higher than pK_a of DCF and pH_{pzc}. Furthermore, H₂O₂ decomposition to O₂ and H₂O at the higher pH (*i.e.* Eq. (8)) [56] and lower oxidation ability of

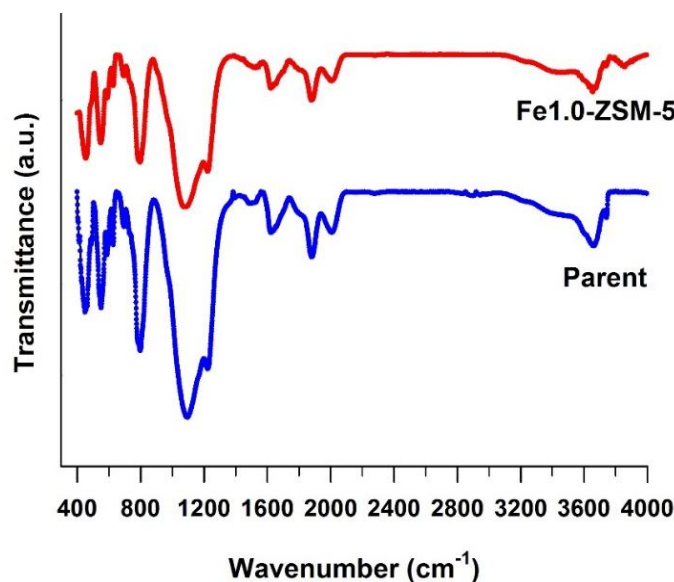


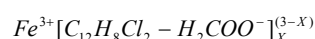
Fig. 6. FT-IR spectra of the catalysts in the range of 400-4000 cm^{-1} .

OH^\bullet are considered responsible for the reduction of the removal efficiency in Fenton reaction in near neutral and alkaline pH levels [57].



Effect of catalyst concentration. The low catalyst concentration favors DCF removal efficiency (Fig. 9). This result can be explained by appropriate availability of the active sites for OH^\bullet production through Eq. (1) [58-60]. The high catalyst concentration ($>2 \text{ g l}^{-1}$) decreases DCF removal which results from the increasing rate of H_2O_2 decomposition (*i.e.* Eq. (8)) owing to mass transfer and thermodynamic limitation [61]. Furthermore, the reaction of the produced hydroxyls with Fe is a side reaction in the Fenton system [62] and OH^\bullet radicals can be subjected to quenching in the presence of the excessive amounts of Fe [59]. These results are in accordance with results of Zhang *et al.* [63] for studying CuFeO_2 as a heterogeneous Fenton catalyst for degradation of bisphenol. They reported that in their proposed system, any increase of CuFeO_2 more than 1.5 g l^{-1} leads to decrease in efficiency of system. In this study, DCF removal experiment by using no amount of the catalyst has only 12% efficiency which clearly highlights the key role of the catalyst in DCF removal. This partial removal is attributed to oxidation of DCF by H_2O_2 .

Effect of H_2O_2 concentration. Effect of H_2O_2 concentration in reaction medium as Fenton reagent is a key parameter. Figure 10 shows the removal efficiency using different amounts of H_2O_2 . Increasing the H_2O_2 concentration reduces DCF removal. Bae *et al* [3] found that addition of H_2O_2 in Fenton degradation of DCF over pyrite led to the saturation pattern in DCF degradation. This phenomenon can be explained by the enhancement of OH^\bullet formation by the addition of H_2O_2 up to the certain level and after that, the excessive amounts of H_2O_2 in the reaction medium act as scavenger and react with generated OH^\bullet (*i.e.* Eq. (5)). It is reported that the formed OH_2^\bullet is less reactive compared with OH^\bullet [64,65]. It is obvious from Fig. 10 that the removal rate is considerably fast in the first 15 min of reaction over the Fe1.0-ZSM-5 catalyst and afterwards it decreases and reaches a steady state. This trend is attributed to formation of the highly stable complexes of Fe^{3+} with by-products of initial degradation or deprotonated ethanoic functional groups:



[2,65]. These highly stable iron complexes inhibit iron regeneration cycle (*i.e.* Eqs. (1)-(2)) [3] and consequently results in the less production of OH^\bullet radicals.

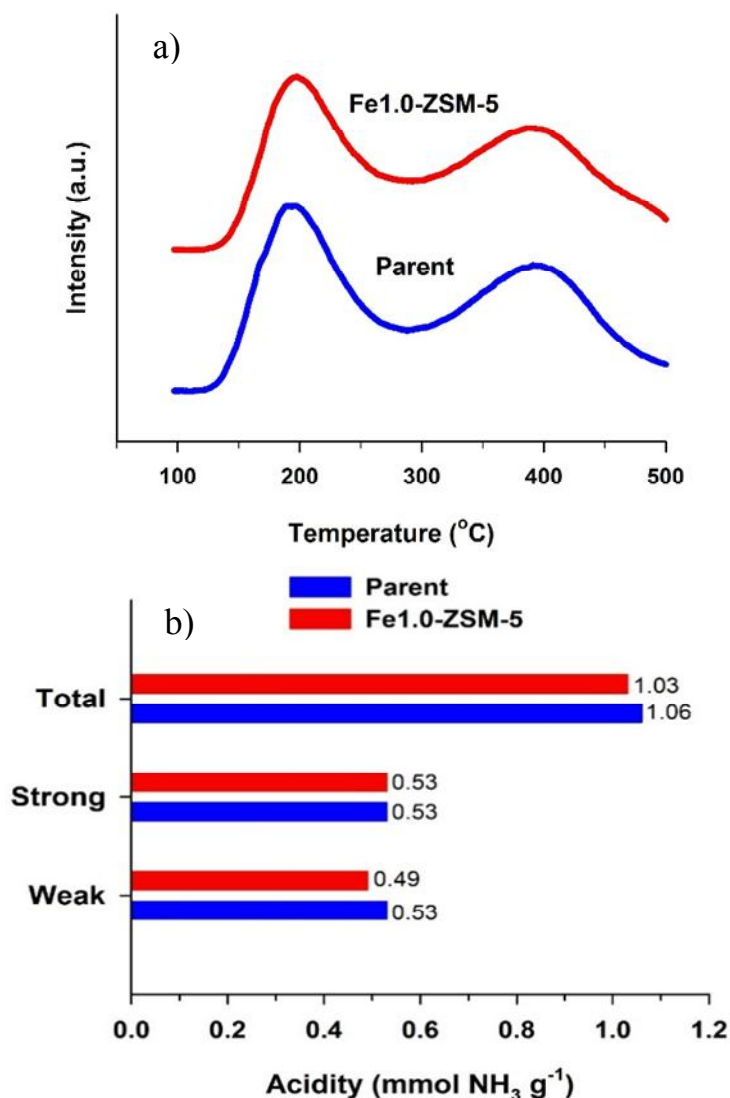


Fig. 7. Acidity properties of the catalysts.

Catalyst Reusability

By applying heterogeneous catalysts in Fenton process, it is possible to separate the used catalyst in further runs. From economical point of view, the applied catalyst would have the high stability and efficiency through the consecutive runs. Figure 11 shows DCF removal efficiency over the catalyst in 4 cycles. After each run, the catalyst is recovered from the final effluent by centrifugation. The regeneration of the catalyst is at 550 °C for 6 h to remove the adsorbed organic species from the catalyst active sites. Catalyst performance for DCF removal drops around 15%

after first cycle, which could be due to leaching of not fully immobilized iron species from zeolite particles. However, DCF removal drops slowly after the second run and changes are in reasonable range for considering the synthesized Fe1.0-ZSM-5 catalyst as reusable Fenton catalyst. The catalyst recovers the active sites through the regeneration process which results in an acceptable efficiency of the catalyst in the second and third cycles (>80%). This phenomenon can be explained by the high specific surface area and total pore volume of the catalyst which enhance the exit of pollutant from the pores and reactivation of the

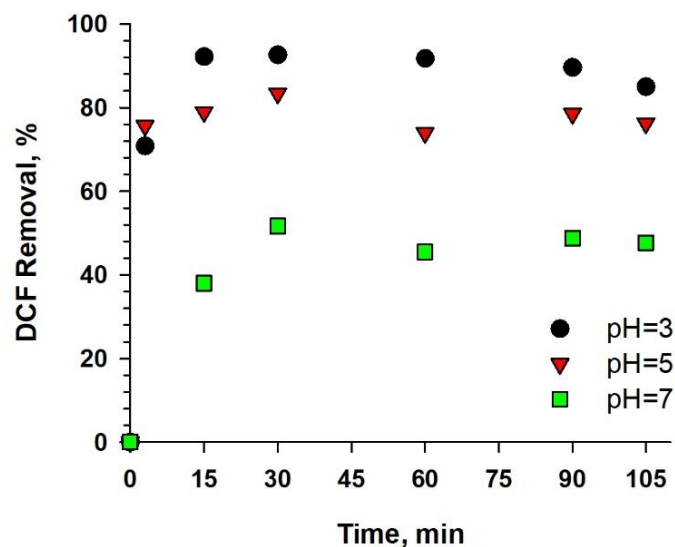


Fig. 8. DCF removal efficiency at different pH levels. Reaction conditions: 2 g l^{-1} , $\text{H}_2\text{O}_2 = 50\text{mM}$, $T = 25 \text{ }^\circ\text{C}$.

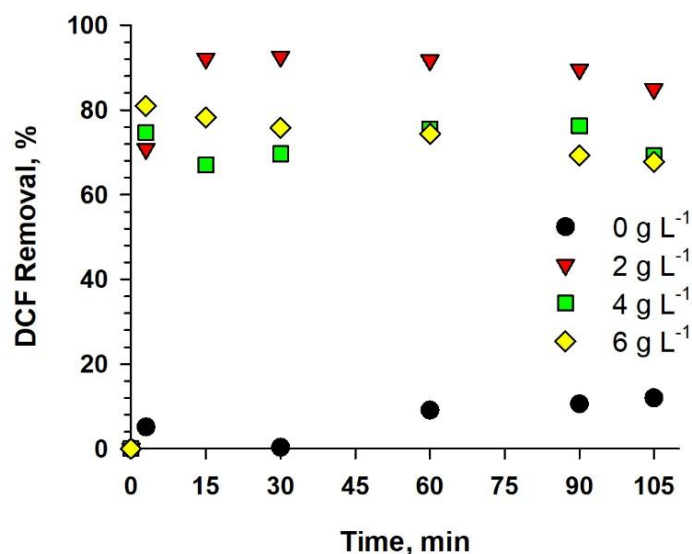


Fig. 9. DCF removal efficiency over different amount of the Fe1.0-ZSM-5 catalyst. Reaction conditions: $\text{H}_2\text{O}_2 = 50 \text{ mM}$, $\text{pH} = 3$, $T = 25^\circ\text{C}$.

active sites. The slightly reduction of the removal efficiency over the regenerated catalyst can be attributed to the poisoning of the active sites owing to the adsorbed organic species, formation of the complexes as well as oxidation of Fe^{2+} to Fe^{3+} . The results confirms the stable performance and the high reusability capacity of the developed catalyst.

CONCLUSIONS

In the present study, heterogenous zeolite catalyst was synthesized by hydrothermal method and impregnated with Fe promoter. The prepared catalyst had the high crystallinity, surface area, and total pore volume. The

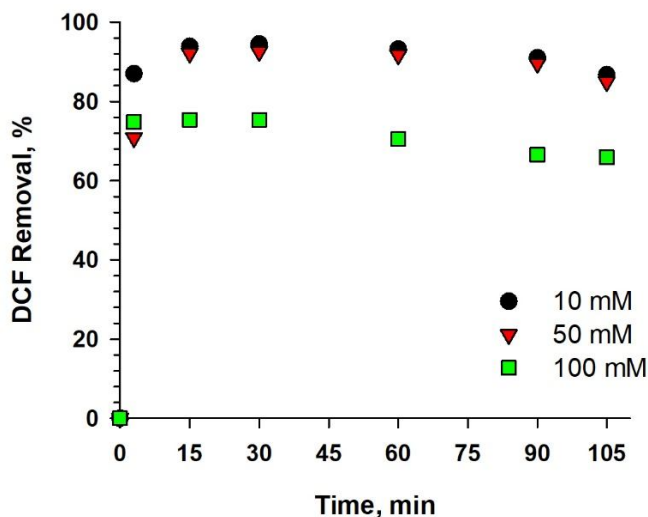


Fig. 10. DCF removal efficiency at different H₂O₂ concentrations. Reaction conditions: 2 g l⁻¹, pH = 3, T = 25°C.

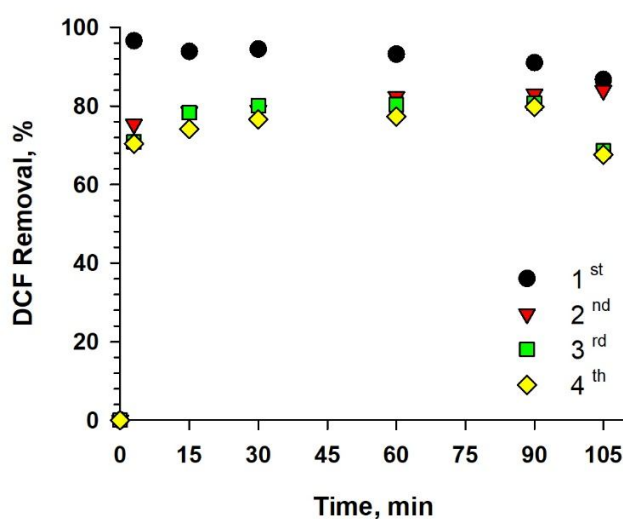


Fig. 11. Reusability of the Fe1.0-ZSM-5 catalyst in DCF removal. Reaction conditions: 2 g l⁻¹, H₂O₂ = 10 mM, pH = 3, T = 25°C.

catalytic performance was investigated under different reaction conditions (pH, temperature, catalyst concentration, and H₂O₂ concentration) for DCF removal through heterogeneous Fenton process. The results showed that the optimum reaction conditions were reaction temperature of 25 °C, H₂O₂ concentration of 10 mM, pH level of 3, and catalyst concentration of 2 g l⁻¹ which resulted in the highest

DCF removal efficiency (97%) after less than 15 min. The Fe1.0-ZSM-5 catalyst had the high and stable performance as well as reusability capacity for the several consecutive runs. In compare with literature, the prepared catalyst were fast and highly efficient which did not require any addition treatment. The results showed the high potential of the Fe-ZSM-5 catalyst for wastewater treatment.

Declaration of Conflicting Interests

The authors declared no potential conflicts of interest with respect to the research, authorship, and/or publication of this article.

Funding

The authors received no financial support for the research, authorship, and/or publication of this article.

REFERENCES

- [1] Feng, L.; Oturan, N.; Van Hullebusch, E. D.; Esposito, G.; Oturan, M. A., Degradation of anti-inflammatory drug ketoprofen by electro-oxidation: comparison of electro-Fenton and anodic oxidation processes, *Environ. Sci. Pollut. Res.*, **2014**, *21*, 8406-8416, 10.1007/s11356-014-2774-2.
- [2] Perisic, D. J.; Gilja, V.; Stankov, M. N.; Katancic, Z.; Kusic, H.; Stangar, U. L.; Dionysiou, D. D.; Bozic, A. L., Removal of diclofenac from water by zeolite-assisted advanced oxidation processes, *J. Photochem. Photobiol. A: Chem.*, **2016**, *321*, 238-247, 10.1016/j.jphotochem.2016.01.030.
- [3] Bae, S.; Kim, D.; Lee, W., Degradation of diclofenac by pyrite catalyzed Fenton oxidation, *Appl. Catal. B: Environ.*, **2013**, *134*, 93-102, 10.1016/j.apcatb.2012.12.031.
- [4] Schwaiger, J.; Ferling, H.; Mallow, U.; Wintermayr, H.; Negele, R., Toxic effects of the non-steroidal anti-inflammatory drug diclofenac: Part I: histopathological alterations and bioaccumulation in rainbow trout, *Aquat. Toxicol.*, **2004**, *68*, 141-150, 10.1016/j.aquatox.2004.03.014.
- [5] Cleuvers, M., Mixture toxicity of the anti-inflammatory drugs diclofenac, ibuprofen, naproxen, and acetylsalicylic acid, *Ecotoxicol. Environ. Saf.*, **2004**, *59*, 309-315, 10.1016/S0147-6513(03)00141-6.
- [6] Behboudi, A.; Jafarzadeh, Y.; Yegani, R., Polyvinyl chloride/polycarbonate blend ultrafiltration membranes for water treatment, *J. Membr. Sci.*, **2017**, *534*, 18-24, 10.1016/j.memsci.2017.04.011.
- [7] Hazrati, H.; Moghaddam, A. H.; Rostamizadeh, M., The influence of hydraulic retention time on cake layer specifications in the membrane bioreactor: Experimental and artificial neural network modeling, *J. Environ. Chem. Eng.*, **2017**, *5*, 3005-3013, 10.1016/j.jece.2017.05.050.
- [8] Mohan, I.; Yadav, S.; Panchal, H.; Brahmabhatt, S., A Review on Solar still: A simple Desalination Technology to obtain potable water, *Int. J. Ambient Energy*, **2017**, *1-20*, 10.1080/01430750.2017.1393776.
- [9] Ishak, A. R.; Hamid, F. S.; Mohamad, S.; Tay, K. S., Removal of organic matter from stabilized landfill leachate using Coagulation-Flocculation-Fenton coupled with activated charcoal adsorption, *Waste Manage. Res.*, **2017**, *35*, 739-746, 10.1177/0734242x17707572.
- [10] Hazrati, H.; Jahanbakhshi, N.; Rostamizadeh, M., Fouling reduction in the membrane bioreactor using synthesized zeolite nano-adsorbents, *J. Membr. Sci.*, **2018**, *555*, 455-462, <https://doi.org/10.1016/j.memsci.2018.03.076>.
- [11] Vosoughi, M.; Fatehifar, E.; Derafshi, S.; Rostamizadeh, M., High efficient treatment of the petrochemical phenolic effluent using spent catalyst: Experimental and optimization, *J. Environ. Chem. Eng.*, **2017**, *5*, 2024-2031, 10.1016/j.jece.2017.04.003.
- [12] Sabour, M. R.; Lak, M. G.; Rabbani, O., Evaluation of the main parameters affecting the Fenton oxidation process in municipal landfill leachate treatment, *Waste Manage. Res.*, **2011**, *29*, 397-405, 10.1177/0734242x10375332.
- [13] Son, G.; Kim, D. -H.; Lee, J. S.; Kim, H. -I.; Lee, C.; Kim, S. -R.; Lee, H., Synchronized methylene blue removal using Fenton-like reaction induced by phosphorous oxoanion and submerged plasma irradiation process, *J. Environ. Manage.*, **2018**, *206*, 77-84, 10.1016/j.jenvman.2017.10.024.
- [14] Rostamizadeh, M.; Jafarizad, A.; Gharibian, S., High efficient decolorization of Reactive Red 120 azo dye over reusable Fe-ZSM-5 nanocatalyst in Electro-Fenton reaction, *Sep. Purif. Technol.*, **2017**, *192*, 340-347, 10.1016/j.seppur.2017.10.041.
- [15] Oturan, N.; Aravindakumar, C. T.; Olvera-Vargas, H.; Sunil Paul, M. M.; Oturan, M. A., Electro-Fenton oxidation of para-aminosalicylic acid: degradation kinetics and mineralization pathway using Pt/carbon-

- felt and BDD/carbon-felt cells, *Environ. Sci. Pollut. Res.*, **2017**, 10.1007/s11356-017-9309-6.
- [16] Baiju, A.; Gandhimathi, R.; Ramesh, S. T.; Nidheesh, P. V., Combined heterogeneous Electro-Fenton and biological process for the treatment of stabilized landfill leachate, *J. Environ. Manage.*, **2018**, *210*, 328-337, 10.1016/j.jenvman.2018.01.019.
- [17] Ahmadi, M.; Kakavandi, B.; Jaafarzadeh, N.; Babaei, A. A., Catalytic ozonation of high saline petrochemical wastewater using PAC@FeIIIFe2IIIIO4: Optimization, mechanisms and biodegradability studies, *Sep. Purif. Technol.*, **2017**, *177*, 293-303, 10.1016/j.seppur.2017.01.008.
- [18] Li, M.; Zeng, Z.; Li, Y.; Arowo, M.; Chen, J.; Meng, H.; Shao, L., Treatment of amoxicillin by O₃/Fenton process in a rotating packed bed, *J. Environ. Manage.*, **2015**, *150*, 404-411, 10.1016/j.jenvman.2014.12.019.
- [19] Safari, G.; Hoseini, M.; Seyedsalehi, M.; Kamani, H.; Jaafari, J.; Mahvi, A., Photocatalytic degradation of tetracycline using nanosized titanium dioxide in aqueous solution, *Int. J. Environ. Sci. Technol.*, **2015**, *12*, 603-616, 10.1007/s13762-014-0706-9.
- [20] Rahmani, H.; Gholami, M.; Mahvi, A.; Alimohammadi, M.; Azarian, G.; Esrafil, A.; Rahmani, K.; Farzadkia, M., Tinidazole removal from aqueous solution by sonolysis in the presence of hydrogen peroxide, *Bull. Environ. Contam. Toxicol.*, **2014**, *92*, 341-346, 10.1007/s00128-013-1193-2.
- [21] GilPavas, E.; Dobrosz-Gómez, I.; Gómez-García, M. Á., Coagulation-flocculation sequential with Fenton or Photo-Fenton processes as an alternative for the industrial textile wastewater treatment, *J. Environ. Manage.*, **2017**, *191*, 189-197, 10.1016/j.jenvman.2017.01.015.
- [22] Bokare, A. D.; Choi, W., Review of iron-free Fenton-like systems for activating H₂O₂ in advanced oxidation processes, *J. Hazard. Mat.*, **2014**, *275*, 121-135, 10.1016/j.jhazmat.2014.04.054.
- [23] De Heredia, J. B.; Torregrosa, J.; Dominguez, J. R.; Peres, J. A., Kinetic model for phenolic compound oxidation by Fenton's reagent, *Chemosphere*, **2001**, *45*, 85-90, 10.1016/S0045-6535(01)00056-X.
- [24] Azbar, N.; Yonar, T.; Kestioglu, K., Comparison of various advanced oxidation processes and chemical treatment methods for COD and color removal from a polyester and acetate fiber dyeing effluent, *Chemosphere*, **2004**, *55*, 35-43, 10.1016/j.chemosphere.2003.10.046.
- [25] Kwan, W. P.; Voelker, B. M., Rates of hydroxyl radical generation and organic compound oxidation in mineral-catalyzed Fenton-like systems, *Environ. Sci. Technol.*, **2003**, *37*, 1150-1158, 10.1021/es020874g.
- [26] Azizi, A.; Moghaddam, M. A.; Maknoon, R.; Kowsari, E., Innovative combined technique for high concentration of azo dye AR18 wastewater treatment using modified SBR and enhanced Fenton process as post treatment, *Process Saf. Environ. Prot.*, **2015**, *95*, 255-264, 10.1016/j.psep.2015.03.012.
- [27] Jafarizad, A.; Rostamizadeh, M.; Zarei, M.; Gharibian, S., Mitoxantrone removal by electrochemical method: A comparison of homogenous and heterogenous catalytic reactions, *Environ. Health Eng. Manage. J.*, **2017**, *4*, 185-193, 10.15171/EHEM.2017.26.
- [28] Munoz, M.; de Pedro, Z. M.; Casas, J. A.; Rodriguez, J. J., Preparation of magnetite-based catalysts and their application in heterogeneous Fenton oxidation-a review, *Appl. Catal. B: Environ.*, **2015**, *176*, 249-265, 10.1016/j.apcatb.2015.04.003.
- [29] Zhang, J.; Sui, Q.; Li, K.; Chen, M.; Tong, J.; Qi, L.; Wei, Y., Influence of natural zeolite and nitrification inhibitor on organics degradation and nitrogen transformation during sludge composting, *Environ. Sci. Pollut. Res.*, **2017**, *24*, 9122-9122, 10.1007/s11356-017-8918-4.
- [30] Garrido-Ramirez, E.; Marco, J.; Escalona, N.; Ureta-Zanartu, M., Preparation and characterization of bimetallic Fe-Cu allophane nanoclays and their activity in the phenol oxidation by heterogeneous electro-Fenton reaction, *Microporous Mesoporous Mater.*, **2016**, *225*, 303-311, 10.1016/j.micromeso.2016.01.013.
- [31] Trapido, M.; Epold, I.; Dulova, N., Degradation of diclofenac in aqueous solution by homogeneous and heterogeneous photolysis, *J. Environ. Eng. Ecol. Sci.*, **2012**, *1*, 1-8, 10.7243/2050-1323-1-3.
- [32] Salaeh, S.; Perisic, D. J.; Biosic, M.; Kusic, H.; Babic, S.; Stangar, U. L.; Dionysiou, D. D.; Bozic, A. L.,

- Diclofenac removal by simulated solar assisted photocatalysis using TiO₂-based zeolite catalyst; mechanisms, pathways and environmental aspects, *Chem. Eng. J.*, **2016**, 304, 289-302, 10.1016/j.cej.2016.06.083.
- [33] Rostamizadeh, M.; Yaripour, F.; Hazrati, H., Ni-doped high silica HZSM-5 zeolite (Si/Al=200) nanocatalyst for the selective production of olefins from methanol, *J. Anal. Appl. Pyrolysis*, **2018**, 132, 1-10, <https://doi.org/10.1016/j.jaap.2018.04.003>.
- [34] Rostamizadeh, M.; Yaripour, F.; Hazrati, H., High efficient mesoporous HZSM-5 nanocatalyst development through desilication with mixed alkaline solution for methanol to olefin reaction, *J. Porous Mater.*, **2018**, 25, 1287-1299, 10.1007/s10934-017-0539-2.
- [35] Rostamizadeh, M.; Yaripour, F., Bifunctional and bimetallic Fe/ZSM-5 nanocatalysts for methanol to olefin reaction, *Fuel*, **2016**, 181, 537-546, 10.1016/j.fuel.2016.05.019.
- [36] Valdés, H.; Tardón, R. F.; Zaror, C. A., Role of surface hydroxyl groups of acid-treated natural zeolite on the heterogeneous catalytic ozonation of methylene blue contaminated waters, *Chem. Eng. J.*, **2012**, 211-212, 388-395, 10.1016/j.cej.2012.09.069.
- [37] Guiza, S., Biosorption of heavy metal from aqueous solution using cellulosic waste orange peel, *Ecol. Eng.*, **2017**, 99, 134-140.
- [38] Baerlocher, C.; McCusker, L. B.; Olson, D. H., Atlas of Zeolite Framework Types, Access Online via Elsevier, 2007.
- [39] Rebrov, E. V.; Seijger, G. B. F.; Calis, H. P. A.; de Croon, M. H. J. M.; van den Bleek, C. M.; Schouten, J. C., The preparation of highly ordered single layer ZSM-5 coating on prefabricated stainless steel microchannels, *Appl. Catal. A*, **2001**, 206, 125-143, 10.1016/S0926-860X(00)00594-9.
- [40] Chen, L.; Zhu, S. Y.; Wang, Y. M.; He, M. -Y., One-step synthesis of hierarchical pentasil zeolite microspheres using diamine with linear carbon chain as single template, *New J. Chem.*, **2010**, 34, 2328-2334, 10.1039/C0NJ00316F.
- [41] Mahboub, M. J. D.; Ahmadpour, A.; Rashidi, H., Improving methane storage on wet activated carbons at various amounts of water, *J. Fuel Chem. Technol.*, **2012**, 40, 385-389, 10.1016/S1872-5813(12)60017-6.
- [42] Serrano, D. P.; Pinnavaia, T. J.; Aguado, J.; Escola, J. M.; Peral, A.; Villalba, L., Hierarchical ZSM-5 zeolites synthesized by silanization of protozeolitic units: Mediating the mesoporosity contribution by changing the organosilane type, *Catal. Today*, **2014**, 227, 15-25, <http://dx.doi.org/10.1016/j.cattod.2013.10.052>.
- [43] Darabi Mahboub, M. J.; Rostamizadeh, M.; Dubois, J. -L.; Patience, G. S., Partial oxidation of 2-methyl-1,3-propanediol to methacrylic acid: experimental and neural network modeling, *RSC Adv.*, **2016**, 6, 114123-114134, 10.1039/C6RA16605A.
- [44] Cabral de Menezes, S. M.; Lam, Y. L.; Damodaran, K.; Pruski, M., Modification of H-ZSM-5 zeolites with phosphorus. 1. Identification of aluminum species by ²⁷Al solid-state NMR and characterization of their catalytic properties, *Microporous Mesoporous Mater.*, **2006**, 95, 286-295, 10.1016/j.micromeso.2006.05.032.
- [45] Rostamizadeh, M.; Yaripour, F., Dealumination of high silica H-ZSM-5 as long-lived nanocatalyst for methanol to olefin conversion, *J. Taiwan Inst. Chem. Eng.*, **2017**, 71, 454-463, 10.1016/j.jtice.2016.12.003.
- [46] Campbell, S. M.; Jiang, X. -Z.; Howe, R. F., Methanol to hydrocarbons: spectroscopic studies and the significance of extra-framework aluminium, *Microporous Mesoporous Mater.*, **1999**, 29, 91-108, 10.1016/S1387-1811(98)00323-0.
- [47] Rostamizadeh, M.; Taeb, A., Synthesis and characterization of HZSM-5 catalyst for methanol to propylene (MTP) reaction, *Synth. React. Inorg., Met.-Org., Nano-Met. Chem.*, **2016**, 46, 665-671, 10.1080/15533174.2014.988825.
- [48] Sun, Y.; Yan, H.; Liu, D.; Zhao, D., A comparative study on the dehydration of monoethanolamine over cesium phosphate modified zeolite catalysts, *Catal. Commun.*, **2008**, 9, 924-930, 10.1016/j.catcom.2007.09.021.
- [49] Kustov, L. M.; Kazansky, V. B.; Ratnasamy, P., Spectroscopic investigation of iron ions in a novel ferrisilicate pentasil zeolite, *Zeolites*, **1987**, 7, 79-83, 10.1016/0144-2449(87)90125-4.

- [50] Ayoub, H.; Roques-Carmes, T.; Potier, O.; Koubaissy, B.; Pontvianne, S.; Lenouvel, A.; Guignard, C.; Mousset, E.; Poirot, H.; Toufaily, J., Iron-impregnated zeolite catalyst for efficient removal of micropollutants at very low concentration from Meurthe river, *Environ. Sci. Pollut. Res.*, **2018**, 1-18, 10.1007/s11356-018-1214-0.
- [51] Stumm, W.; Morgan, J. J., *Aquatic Chemistry: Chemical Equilibria and Rates in Natural Waters*, John Wiley & Sons, 2012.
- [52] Zhang, H.; Choi, H. J.; Huang, C. -P., Optimization of Fenton process for the treatment of landfill leachate, *J. Hazard. Mater.*, **2005**, *125*, 166-174, 10.1016/j.jhazmat.2005.05.025.
- [53] Trovó, A. G.; Nogueira, R. F., Diclofenac abatement using modified solar photo-Fenton process with ammonium iron(III) citrate, *J. Braz. Chem. Soc.*, **2011**, *22*, 1033-1039, 10.1590/S0103-50532011000600005
- [54] Larous, S.; Meniai, A. -H., Adsorption of Diclofenac from aqueous solution using activated carbon prepared from olive stones, *Int. J. Hydrogen Energy*, **2016**, *41*, 10380-10390.
- [55] Neamtu, M.; Catrinescu, C.; Kettrup, A., Effect of dealumination of iron(III)-exchanged Y zeolites on oxidation of Reactive Yellow 84 azo dye in the presence of hydrogen peroxide, *Appl. Catal. B: Environ.*, **2004**, *51*, 149-157, 10.1016/j.apcatb.2004.01.020.
- [56] Ahmed, Y.; Yaakob, Z.; Akhtar, P., Degradation and mineralization of methylene blue using a heterogeneous photo-Fenton catalyst under visible and solar light irradiation, *Catal. Sci. Technol.*, **2016**, *6*, 1222-1232, 10.1039/C5CY01494H.
- [57] Pignatello, J. J.; Oliveros, E.; MacKay, A., Advanced oxidation processes for organic contaminant destruction based on the Fenton reaction and related chemistry, *Crit. Rev. Environ. Sci. Technol.*, **2006**, *36*, 1-84, 10.1080/10643380500326564.
- [58] Ramirez, J. H.; Maldonado-Hódar, F. J.; Pérez-Cadenas, A. F.; Moreno-Castilla, C.; Costa, C. A.; Madeira, L. M., Azo-dye Orange II degradation by heterogeneous Fenton-like reaction using carbon-Fe catalysts, *Appl. Catal. B: Environ.*, **2007**, *75*, 312-323, 10.1016/j.apcatb.2007.05.003.
- [59] Singh, L.; Rekha, P.; Chand, S., Cu-impregnated zeolite Y as highly active and stable heterogeneous Fenton-like catalyst for degradation of Congo red dye, *Sep. Purif. Technol.*, **2016**, *170*, 321-336, 10.1016/j.seppur.2016.06.059.
- [60] Rache, M. L.; García, A. R.; Zea, H. R.; Silva, A. M.; Madeira, L. M.; Ramírez, J. H., Azo-dye orange II degradation by the heterogeneous Fenton-like process using a zeolite Y-Fe catalyst-kinetics with a model based on the Fermi's equation, *Appl. Catal. B: Environ.*, **2014**, *146*, 192-200.
- [61] Andas, J.; Adam, F.; Rahman, I. A., Heterogeneous copper-silica catalyst from agricultural biomass and its catalytic activity, *Appl. Surf. Sci.*, **2013**, *284*, 503-513.
- [62] Hou, B.; Han, H.; Jia, S.; Zhuang, H.; Xu, P.; Wang, D., Heterogeneous electro-Fenton oxidation of catechol catalyzed by nano-Fe₃O₄: kinetics with the Fermi's equation, *J. Taiwan Inst. Chem. Eng.*, **2015**, *56*, 138-147, 10.1016/j.jtice.2015.04.017.
- [63] Zhang, X.; Ding, Y.; Tang, H.; Han, X.; Zhu, L.; Wang, N., Degradation of bisphenol a by hydrogen peroxide activated with CuFeO₂ microparticles as a heterogeneous Fenton-like catalyst: efficiency, stability and mechanism, *Chem. Eng. J.*, **2014**, *236*, 251-262, 10.1016/j.cej.2013.09.051.
- [64] Zhan, Y.; Li, H.; Chen, Y., Copper hydroxyphosphate as catalyst for the wet hydrogen peroxide oxidation of azo dyes, *J. Hazard. Mater.*, **2010**, *180*, 481-485, 10.1016/j.jhazmat.2010.04.055.
- [65] Kušić, H.; Koprivanac, N.; Selanec, I., Fe-exchanged zeolite as the effective heterogeneous Fenton-type catalyst for the organic pollutant minimization: UV irradiation assistance, *Chemosphere*, **2006**, *65*, 65-73, 10.1016/j.chemosphere.2006.02.053.